Sensing and Bio-Sensing Research 37 (2202) 100505

Contents lists available at ScienceDirect

Sensing and Bio-Sensing Research

journal homepage: www.elsevier.com/locate/sbsr

Portable flow multiplexing device for continuous, *in situ* biodetection of environmental contaminants

J.-Pablo Salvador [a,b], M.-Pilar Marco [a,b], Giacomo Saviozzi [c], Cecilia Laschi [c], Fernando Arreza [d], Francisco Palacio [d], Manel Lopez [d,*]

[a] *Nanobiotechnology for diagnostics (Nb4D), Department of Chemical and Biomolecular Nanotechnology, Institute for Advanced Chemistry of Catalonia (IQAC) of the Spanish Council for Scientific Research (CSIC), Barcelona, Spain*
[b] *CIBER de Bioingeniería, Biomateriales y Nanomedicina (CIBER-BBN), Jordi Girona 18-26, E-08034 Barcelona, Spain*
[c] *Marine Robotics, The BioRobotics Institute, Scuola Superiore Sant'Anna (SSSA), 56025 Pontedera, Italy*
[d] *Departament d'Enginyeria Electrònica i Biomèdica, Universitat de Barcelona, C/ Martí i Franquès 1, E-08028 Barcelona, Spain*

ARTICLE INFO

Keywords:
Environmental monitoring
Amperometric biosensors
Pollutants
Pulsing flow method
Low-power and low-cost biosensing platform

ABSTRACT

A compact, low-cost and low-powered device was developed and arranged for multiplexed biodetection of sea water contaminants from continuous flow mode. Electronics, mechanics and fluidics were designed to guarantee identical functional liquid flow through eight parallel sensor microchambers during a predetermined time period providing 8 values at the same time. The accuracy and repeatability of the device was tested in-lab, achieving a deviation of less than 10% when measuring the same analyte in all the chambers. The experimental results obtained with our device were finally compared with those measured in continuous flux by a commercial potentiostat SP150 (Bio-Logic Science Instruments), obtaining identical results, which validated the proposed device.

1. Introduction

Marine regions account for over 40% of Europe's gross domestic product (GDP) [1], being between 3 and 5% of the latter generated directly from marine-based services and industries [2,3]. Moreover, the direct impact of marine resources on quality of life, public health and business development is of utmost value despite being non-quantifiable. Proof of this impact is that EU aquaculture production reached 1.2 million tons of seafood in 2020 and a sale value of € 4.1 billion in turnover in 2018 [2,4,5] (These reports estimate that the coronavirus pandemic hit the sector by decreasing income sources and increasing costs). In this context, chemical contamination of estuarine and coastal areas carries perverse consequences for the environment and through the food chain for public health. In addition, coastal industries (*e.g.* fisheries) are already being severely affected.

According the European Commission (EC) through specific scientific committee on food, farming and fisheries [5] promoted policies to ensure food quality and safety in agriculture/aquaculture products. They have special interest to include severe limitations on the use of chemical products, spills and usage of facilities for food safety. In this context, EC sponsors every year many scientific projects for developing technological solutions to face this issue, and created a permanent project calls, specific for marine and coastal issues. Some of these scientific and technical projects involve developing early warning systems that provide extreme sensitive and selective data for monitoring sea water and eventually triggering an alarm in case the level of contamination reaches a meaningful threshold. This work was carried out within the framework of the **Sea-on-a-chip** project (FP7-OCEAN614168) and aimed to develop a miniaturized, autonomous, remote and flexible immunosensor platform for real-time monitoring of marine waters in multi-stressor conditions by providing a concrete application for aquaculture facilities. The immunosensor platform was based on a fully integrated array of microelectrodes with electrochemical detection (amperometric) and a microfluidic system in a lab-on-a-chip-like configuration.

Current analytical techniques for the detection of environmental pollutants are based on chromatographic techniques coupled to mass spectrometric detectors in centralized laboratories [6]. These methods are characterized with high detectability, specificity, multianalyte analysis and are considered as the golden standard methodology for the

* Corresponding author.
E-mail address: manel.lopez@ub.edu (M. Lopez).

https://doi.org/10.1016/j.sbsr.2022.100505
Received 22 February 2022; Received in revised form 19 May 2022; Accepted 31 May 2022
Available online 3 June 2022

validation and confirmatory method of screening techniques. However, they require preconcentration and clean-up strategies, qualified personnel and complex instrumentation that results in a high cost/analysis ratio. In order to reach enough detectability to monitor on-time environmental pollutant, it is required develop rapid, simple and low-cost devices.

Immunosensors make use of the specific binding between an antibody and antigen coupled to physical transducer that converts the bio-recognition process into measurable signal [7]. The antigen-antibody interaction is the basis of a wide variety of immunochemical methods enough selective and sensitive to detect organic pollutants. Indeed, immunoassays have been widely used in environmental applications [8] as a high throughput method allowing the simultaneous analysis of a number of samples. These can be adapted to rapid detection formats such as dip-sticks or presented in combination with transducer elements to develop immunosensors [9]. Electrochemical immunosensors have gained attention due to their high detectability, robustness and simplicity in the design of the electrodes, specifically better using amperometric techniques. According to these advantages, the development of an autonomous and automatic device based on this transducing principle was one of the challenges that are facing in this work.

Electrochemical biosensors are commonly assembled for point-of-care applications due to its rapid analytical response, its possibility of miniaturization, that implies a reduction in size and power consumption. Finally, it is important to remark their ability to perform analysis on the field. Some immunosensor platform architectures have been reported in the literature, in both the environmental [10–12] and biomedical [13–18] contexts. Automated, on time and *in situ* environmental chemical sensors and point-of-care systems have led out alternatives to traditional manual sampling (which also involves preservation and transportation to a laboratory for further analysis, at the risk of sample degradation and/or contamination), in all cases the microfluidic technology is the fundamental requirement. In this context, automated sampling and on time, *in situ* analysis not only overcomes the risk of sample damage and cumbersome logistics, but also allows for high measurement frequency or continuous measurement in remote locations (*e.g.*, open seas). Moreover, this microfluidics-based strategy plays an important role in the accuracy achieved in some *in situ* chemical measurements; this is the case of some chemical parameters that contrary to pH, oxygen or nitrate, cannot be measured with solid state sensors [19–26]. In some cases, the sample needs chemical pre-treatment prior to being presented to a chemical sensor (*e.g.*, to measure the concentration of a determined chemical pollutant). The use of microfluidics in such cases helps increase the operational lifetime of *in situ* chemical sensors by carefully managing the reagent stock and pumping energy [27–30].

Energy storage is precisely one of the most challenging issues in the management of automated *in situ* environmental sensing systems and point-of-care technology. Although much progress has been made during the past years in terms of energy management, there is still a long way ahead to achieve highly efficient systems whilst maintaining analytical performances. The pumping action is one of the most critical influences in energy efficiency since it must be supplied with a considerable power level. In this work, a pulsed flow mechanism is presented for the first time to the authors' knowledge as a suitable method for reducing power consumption in an autonomous and *in situ* sensor network for analysis of sea water pollutants. Here, the complete system is described in several parts, comprising the microfluidics and multiplexing of fluid towards the electrochemical sensor array, the electronics and hardware for micropumps and microvalves control and sample analysis and the software for remote control with a graphical user interface. As a proof of concept, the determination of marine pollutants using antibodies was proposed in this work. Specifically, the demonstration was performed using immunoreagents for the determination of Irgarol 1051® [32].

2. The measurement system

The measurement system designed for detecting marine contaminants is a complex device that allow us to monitor in a continuous way up to eight different contaminants simultaneously. To do this, it incorporates an important electromechanical and microfluidic part coupled with an electronic control system that manage the whole device, including the liquids dispensing protocol and the measurement algorithm. To perform the liquids dispensing in the different biosensor's micro-chambers a fluidic module was done in an integrated way, using CAD tools for the complete mechanical design of the prototype. The schematic design of the whole system, different pictures that show the electronic, the electromechanical and microfluidical stage and the power consumption analysis are presented throughout this paper. The final prototype, including schematics, software flux diagrams and other characteristics are available in the supplementary material. This supplementary material also includes a video (SM Video_1) that shows the functionality of the whole platform.

The different blocks that make up the measurement system are described in detail below.

2.1. Immunosensor protocol

This paragraph is focused on the design of an innovative immunoassay flow multiplexing system capable of detecting and quantifying up to eight parallel analytes in an autonomous way. For this purpose, we selected the immunoreagent pair 4e-BSA/As87 (4e-BSA: Bovine serum albumin coupled to a Hapten 4e; Hapten: molecule that mimic the target analyte to be coupled to a carrier protein to induce immune response; As87: antiserum specific for Irgarol 1051®) required for the detection of Irgarol 1051®. This contaminant has been studied widely in our laboratory in different formats such as ELISA [34–36,46], fluorescent microarray [37], optical [38,39] and electrochemical immunosensors [32,33]. Irgarol 1051® is a triazine herbicide that is being used as antifouling paint on recreational and commercial watercraft hulls to prevent algae growth. In our case, the measurement and detection of this contaminant requires the use of a well functionalized electrochemical immunosensor and the implementation of a competitive assay protocol. Such competitive assay protocol is summarized in Fig. 1. Basically, the detection of small molecules such as Irgarol 1051® requires the immobilization of the competitor (4e-BSA) on the chip's sensor surface and then incubate the specific antibody and the sample that contains the pollutant. After a period of incubation, the remaining antibody untied to the analyte is removed by a washing step. In order to acquire the binding competitor-antibody, a secondary antibody labeled with anti-IgG Horseradish Peroxidase conjugate (aHRP) is added. HRP would provide the electrochemical signal after the addition the corresponding substrate (H_2O_2/TMB -Hydrogen Peroxide/Tetramethylbenzidine-based solution). Once the measurements have been performed, the chip can be regenerated after the addition the NaOH 0.3 M solution to be ready for the next simultaneous measurements.

According to this protocol a number of tanked reagents linked to the microfluidic system are required. This is depicted in Fig. 2, where a scheme of the mixture and measurement flow pathways, including the required peristaltic micropumps and microvalves necessary to perform the process, is shown. Basically, it requires a tank containing Phosphate Buffered Saline buffer with Tween® 20 (PBST) to perform both the washes between stages and the conditioning of the biosensor chambers. The Antibody buffer (ABB) tank supplies the specific antibodies for the recognition of the target analyte. The sample is pushed and addressed to the Dilution tank (DT) by a peristaltic micropump, where it is combined with the antibody for the analyte-antibody preincubation. After a period of time defined in Table 1, the content is flooded to the biosensor chambers. To complete the biosensor protocol defined in Fig. 1, the device requires the inclusion of the anti-IgG-HRP conjugate, the detection solution and the regeneration solution, which are stored in the

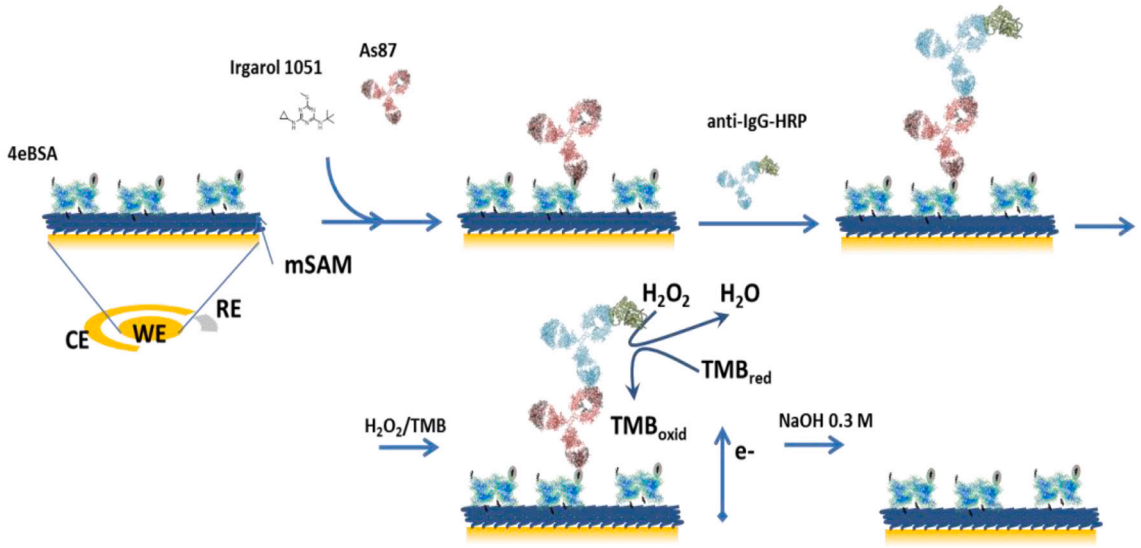

Fig. 1. Immunosensor procedure for the determination of Irgarol 1051®.

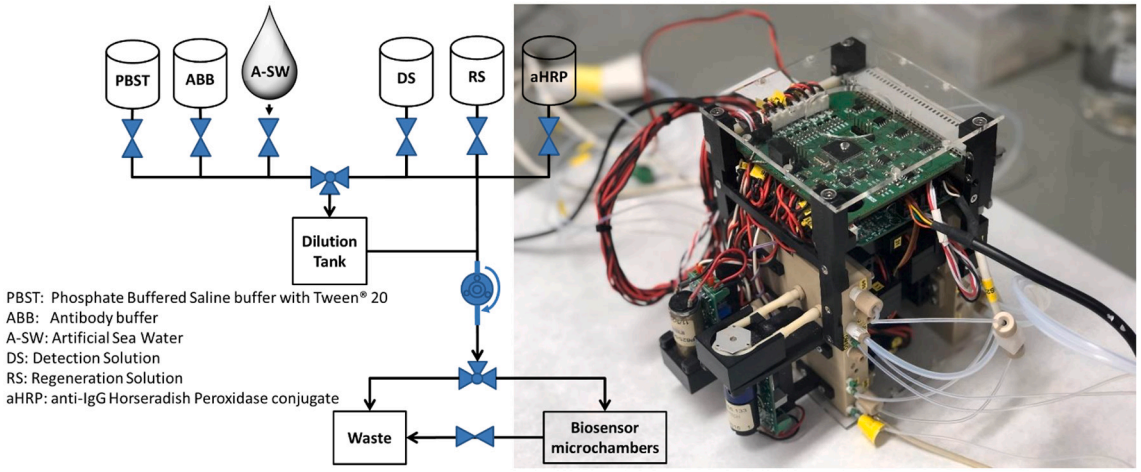

Fig. 2. Schematic of the microfluidic network controlled by peristaltic micropumps and microvalves through which the reagents flow to the biosensor μchambers and eventually to waste. Sample Loading pipe is introduced to perform the measurement. Tanks contain PBST, Detection solution (DS), Regeneration Solution (RS) and the anti-IgG-HRP conjugate solution (aHRP). Fig. 2 also shows a picture of the final device. Dimensions and weight of the prototype were 2175 cm^3 and less than 1 kg.

Table 1
Steps involved for continuous flow *in situ* multiplexed biodetection of the developed device.

Step	Description	Quantity
1	Flood the Mixing with:	7 ml
1.1	Sample from A-SW	6.8 ml
1.2	0.2 ml of antibody (ABB)	0.2 ml
2	Flood the DT content into the Bioensor μchambers	7 ml
3	Flood the DT with PBST for washing	7 ml
4	Use the DT content with PBST to wash the Biosensor μchambers	7 ml
5	Add aHRP content into the biosensor μchamber	5 ml
6	Wash biosensor chambers and pipes with PBST	2 ml
7	Add DS to the biosensors μchambers. Start measuring with Sensor unit (SU)	4 ml
8-	Wash biosensor chambers and pipes with PBST	2 ml
9	Add RS in the biosensor μchamber	10 ml
10	Wash biosensor chambers and pipes with PBST	2 mi

aHRP, detection solution (DS) and regeneration solution (RS) tanks respectively. Finally, a technical issue is important to remark, according to the peristaltic pump used, a minimum flow rate was used and set at 0.027 ml/s in all the steps, to favor the analyte-antibody interaction. Fig. 2 also shows a picture of the final device. As can be observed, the prototype has a compact structure, where all the elements discussed in the previous paragraph have been integrated into a volume of 2175 cm^3 (10.28 × 10.28 × 20.56) and a total weight of less than 1 kg. An immunoassay protocol was designed to perform the device's automation and the steps required are shown in Table 1.

2.2. Dispensing liquids: the pulsed-flow method

The aforementioned amperometric biosensor prepared to measure the Irgarol 1051® concentration was carried out over a commercial array of eight three-electrode biosensors, each with a 2.56 mm-diameter gold-based working electrode (WE), a gold and silver-based counter (CE) and a reference (RE) electrode. It allowed to validate the behavior of our platform. A detailed description and use of both measurement and biosensor is well described in [31,32]. Then, the amperometric measurement process was the transducing principle chosen for the acquisition of the signal. The electrochemical responses from the eight sensor cells are acquired by the detection of the oxidized TMB in the presence of H_2O_2 and HRP. The fact that the electroactive compound (TMB/H_2O_2) is

in solution creates a significant risk of cross-talk between the Screen-Printed Electrodes (SPEs) that are in the same sensor chamber [40], for this reason we performed the measurements in individual biosensor chambers. Multiplexing devices present challenges in device design, fabrication and flexible integration compared with other microscale techniques [41], allowing for greater miniaturization, and, in some cases like the present one, a better performance. Simultaneous detection of multiple analytes was performed by eight biosensors dipped in their corresponding microchamber (μchamber). For this, a pulsing method was implemented to allow an identical amount of functional liquid to flow through each μchamber during a predetermined interval time, that is the same flow rate. The behind concept is the well-known and well-defined idea of time-division-multiplexing (TDM) used in networks and communications theory. In TDM, you transmit and receive

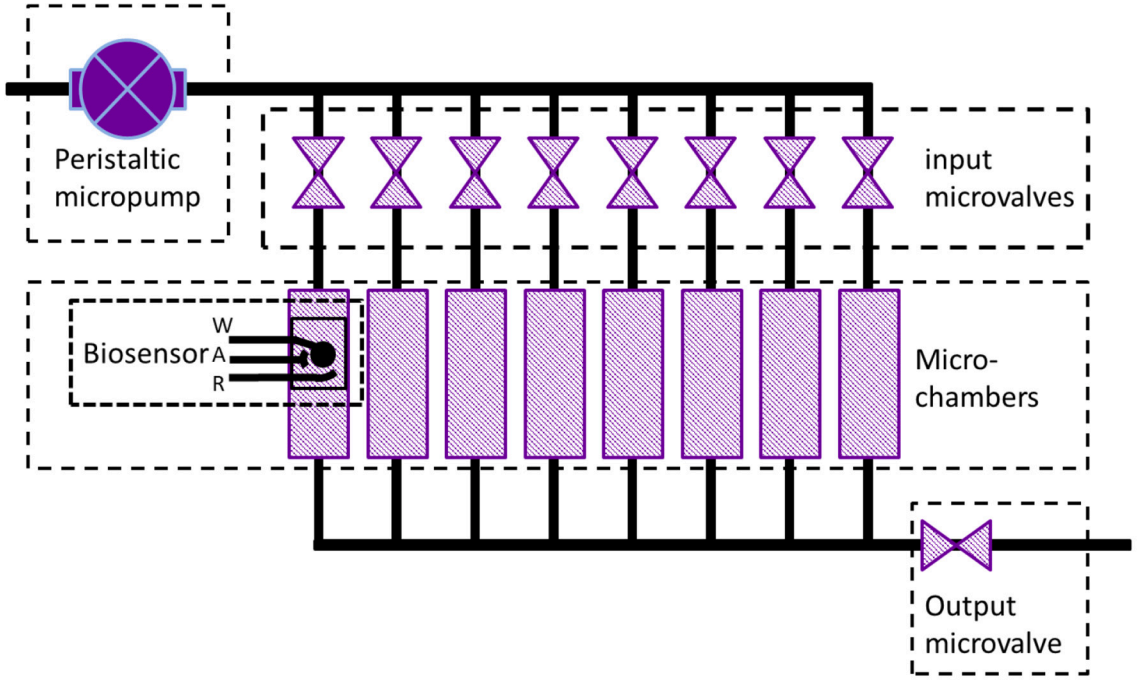

(a)

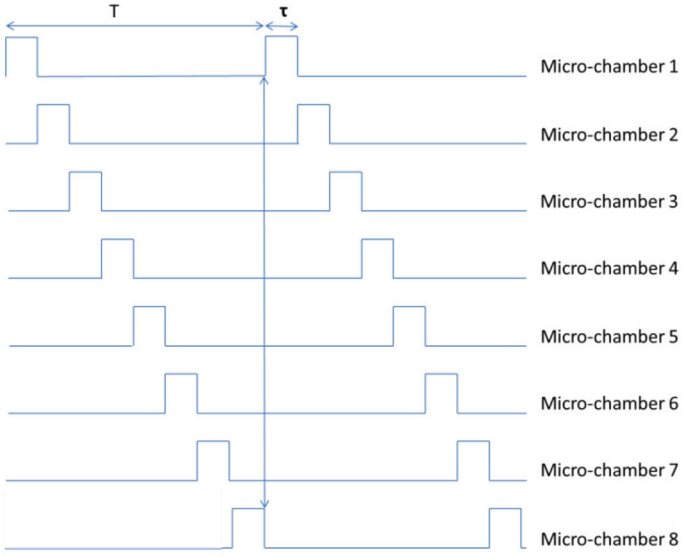

(b)

Fig. 3. a) Detailed schematic of the microfluidic system in the biosensors μchambers. The electrodes biosensor (Working (W), Counter or auxiliary (A) and Reference (R) are included in each Sensor Chamber (SC). There is one input electrovalve for every SC input (eight in total) and one common output electrovalve. b) presents the succession of cyclic flow pulses through the eight-parallel sensor μchambers. The total cyclic period T was one second. The ON period τ was 1 s.

independent code frames from different transmitters to different receivers sharing a common signal path that is synchronized in time, meaning that each transmission frame appears on the common line only a fraction of time in an alternating pattern. Following this concept and adapting it to microfluidics, each biosensor's μchamber (Fig. 3a) is supplied cyclically with equal amount of pulsed functional liquid by a rapid succession of microvalve orifice closure and opening. This succession of flow pulses is schematized in Fig. 3b. There, T is the period in which all the μchambers are flooded with the functional liquid, and is the sum of the flow pulsation time τ performed on every μchamber. Therefore, each chamber during an infinitesimal time period τ is supplied with a flow dQ1 that in the steady state will correspond to a continuous flow of A·v, being A the cross-section area and v the velocity. It means that an identical amount of functional liquid can be outfitted, making them work as if they were supplied in continuous flow mode, even at very low flow rates as long as the liquid is effectively entering the biosensor μchamber. Hence, the μchambers flow rate (and its average value) is identical regardless of the steady peristaltic micropump flow rate, pressure and other parameters of the fluid dynamics.

2.3. Fluidic module

The electrochemical arrays formed by eight screen-printed electrodes (SPE) are specially designed for the development of multiple simultaneous analysis. The biosensor μchamber system, schematically presented in Fig. 3a, consisted of eight individual cells that permit the fitting of this SPE array and perform eight parallel, simultaneous measurements. The physical structure of the sensor chamber was integrated in a 90 mm × 90 mm × 15 mm polyether ether ketone (PEEK) manifold. According to the scheme shown in Fig. 2, two manifolds were designed and constructed to minimize pipes and tubing and reuse common channels, microfluidic pumps and valves. The first one, named Mixing Manifold, contains the Dilution Tank (DT), used to mix the antibodies with the samples. It also includes the inlets from the different tanks presented in Fig. 2. The second manifold was designed to host the microsensor μchambers. The mixture of the inlet sample plus the antibody flood from the DC to each μchamber to perform the measurement according to the process described in section 2.1. Once the measurement has finished, sequentially starts a cleaning process of both manifolds, followed by a regeneration stage, necessary to prepare the sensors to new measurements. In the supplementary material, the whole system is presented, and a video demo (SM: Video_2) of the measurement and cleaning process is included. Fig. 4 shows the mechanical design of both manifolds, and can be appreciated the different cavities, pipes and headers done to minimize the whole system. Both manifolds were designed using the well-known SolidWorks software, a solid modeling computer-aided design from SolidWorks Corporation©. PEEK was chosen for its appropriate chemical and mechanical properties (although it's pretty hard and somehow difficult to work with, PEEK female threads endure several screwing and unscrewing without early crumbling). The diameter of internal connecting pipes was limited to 1/16″ due to drill bit availability. Nine ASCO 2/2 Normally Closed – L S067A 030E microvalves, eight for each μchamber's input and one for whole system cleaning purpose, were connected to the pipes as illustrated in Fig. 3a. The volume of all micro-chambers was identical and equal to ~6mm^3. An Instech P625/900 peristaltic micropump with a power consumption between 25 and 75 mA at 5 V was employed for regulating the flow rate to 1.6 ml/min. All the different parts of the system where interconnected using PharMed 1/16" Internal Diameter (ID) tubing that ensure the functionality of the device. Among the different operating conditions

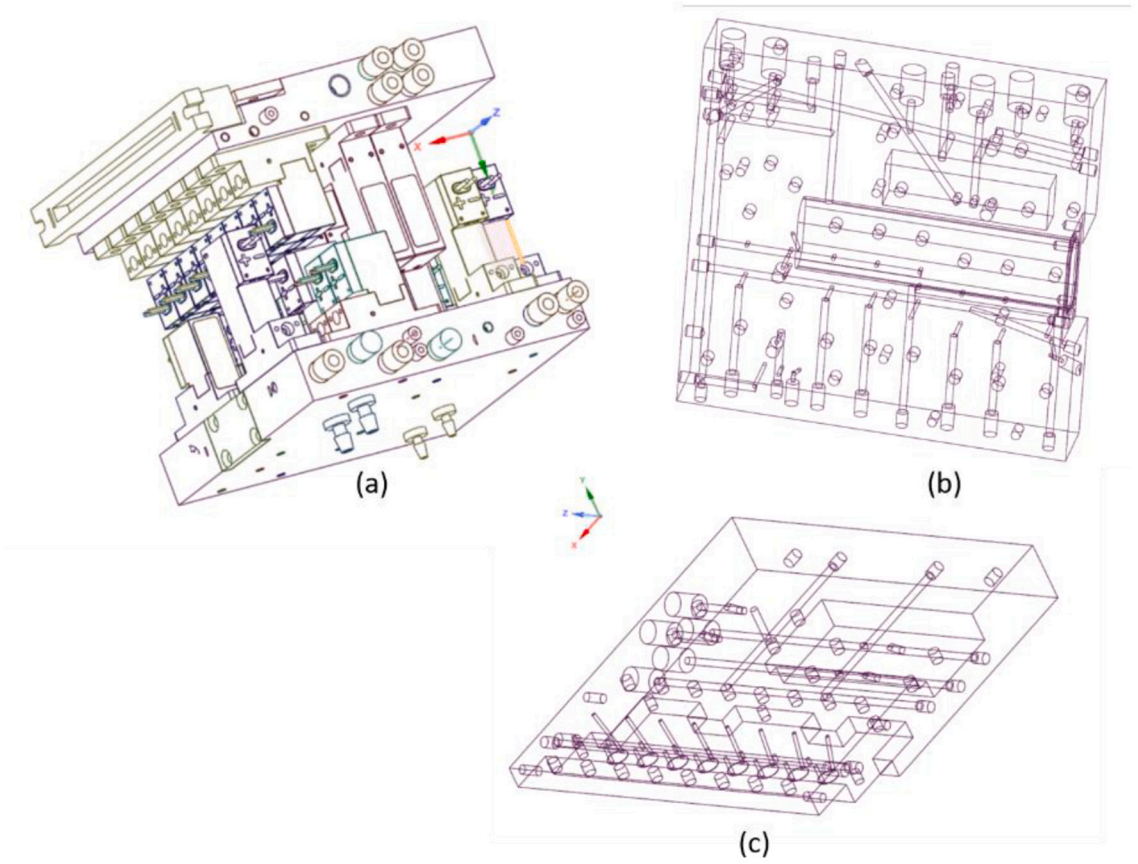

Fig. 4. Mechanical design of the whole system. a) presents the whole system, the two manifolds are at the high and bottom borders of the system. In the middle, between the two manifolds, the different micropumps and microvalves can be appreciated. b) presents the design of the bottom manifold, which includes the dilution tank and the inlets from the different reservoirs. c), the top manifold, shows the sensors μchambers and the interconnection to throw out the mixture.

offered by the peristaltic micropump, the flow rate value of 1.6 ml/min was chosen to completely refill the sensor μchambers, using cyclic pulses of 1 s for each micro-chamber as presented in Figure3b. Finally, the general protocol to perform the measurement implemented in our device is the well-presented and described in Table 1.

2.4. The electronic system

To control a measurement platform as complex as the one proposed in this work, it was necessary to design an electronic system capable of: (i) acting on the different microvalves and micropumps for allowing the introduction, in a controlled manner, of the different chemical compounds into the manifolds to prepare the different solutions; (ii) manage the introduction of the analyte in the μchambers to carry out the measurement and (iii) extract the used up materials from manifolds and μchambers, clean the prototype and regenerate the sensors to be able to carry out the next measurement. Fig. 5 shows a block diagram that presents the main characteristics of the two electronic subsystems that make up the complete electronic system: The excitation signal generator and acquisition electronic subsystem and the central unit subsystem.

The excitation signal and the acquisition electronic subsystem, called henceforth sensor unit (SU), is related with the final measurement, includes the management of the eight inputs microvalves that permits to flow independently the eight sensor chambers, implementing the pulsed-flow method, and perform the measurement. The second one, the central unit (CU), corresponds with the management of the rest of the microvalves and the reservoirs, the filling and emptying of the microchambers, which also includes the activation of the micropump to flow the Mixing Manifold, the power supply system, the communication with the SU and the communication with the user.

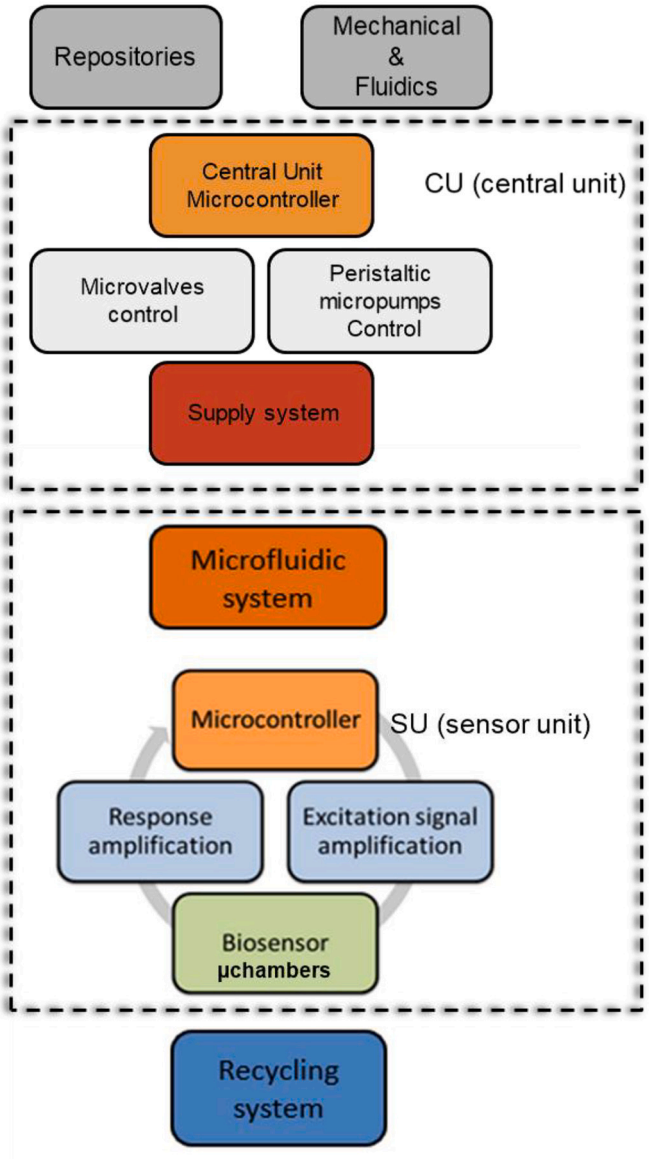

Fig. 5. Block diagram of the whole electronic system.

2.4.1. The sensor unit

The SU is responsible for performing the amperometric measurements of the eight sensors that the system has available. The digital part is based on a 32-bit PIC32MX795F512L (Microchip) microcontroller, in which the management firmware necessary to control the measurement process has been loaded. The analog part is based on a miniaturized potentiostat for measuring amperometric biosensors. Summarizing, the SU has the following tasks: (i) to control the input and output microvalves implementing the pulsed-flow method; (ii) to generate the input voltage signal necessary to excite the sensors; (iii) to acquire the sensing signal using its internal 10 bit analog-to-digital converters (ADC); and (iv) to filter, preprocess and prepare the acquired data before sending them to the CU using a high-speed connection based on CAN 2.0 (Fig. 6).

The activation of the microvalves was done using eight of the microcontroller's digital outputs, which excite the gate of eight RTR020N05 NMOSFET transistors (RHOM), one for every microvalve, allowing the fluids pass to the different sensor μchambers. Schematic design of the SU is shown in the supplementary material (Fig. S4 - S8).

The different sensors were excited with −0.1 V [42] between the reference and the working electrodes using the potentiostat (OPAMP 1 in Fig. 6) based on an OPA2182 (Texas Instruments) operational amplifier. The −0.1 V corresponds to the best signal to be applied to the immobilizer TMB, used as an electron transfer mediator in our amperometric biosensor. Pulse width modulation (PWM) was used to generate this −0.1 V. The signal of the PWM was directly connected to a Sallen-Key low-pass filter, based on an OPA2182, to obtain a clean-of-noise reference (Fig. S6).

The response of the sensor signals was acquired by eight very high input impedance LPC662A OPAMP, configured as transimpedance operational amplifier (TIA). The feedback loops were used for measuring three-lead electrochemical biosensors. The output of this TIA was filtered and directly connected to the microcontroller's Analog to Digital Converter (ADC) inputs (Fig. S7). To perform the *in-situ* signal processing, we took advantage of its 80 MHz, 1.56 DMIPS and Mk4 core with five stage pipeline Harvard architecture (Fig. S4). The complete acquisition electronics is schematized in Fig. 6 and the final PCB design can be observed in Fig. S9. Finally, Fig. S11 shows the embedded firmware flow diagram for the management of the SU, including the communication protocol with the Central Unit.

2.4.2. The central unit

The Central Unit (CU) is responsible of the microfluidics' proper functioning, supply management, synchronization requirements, preparation of the mixture for analyte detection, and respect for cleanliness issues to avoid inter and intra contamination. The digital part of the CU is based on a 32-bit STM32F103ZFT6 (STMicroelectronics) microcontroller, a M3 72 MHz high-performance ARM Cortex M3 processor. The CAN transceiver used in both SU and CU subsystems was the Microchip SN65HVD230D. The analog part of the CU's board includes temperature and humidity sensors (SHT71), a current sensor (INA199) and the driver chosen to control the electrovalves and the micro-pump, the RHOM RTR020N05, the same low resistance n-MOSFET used in the SU. Fig. 7 shows a block diagram of the CU while Fig. S1 shows the PCB design and its integration with the different microfluidic module. The schematic of this system is also shown in the supplementary material (Fig. S2 and S3).

The CU also manages two different serial communication channels.

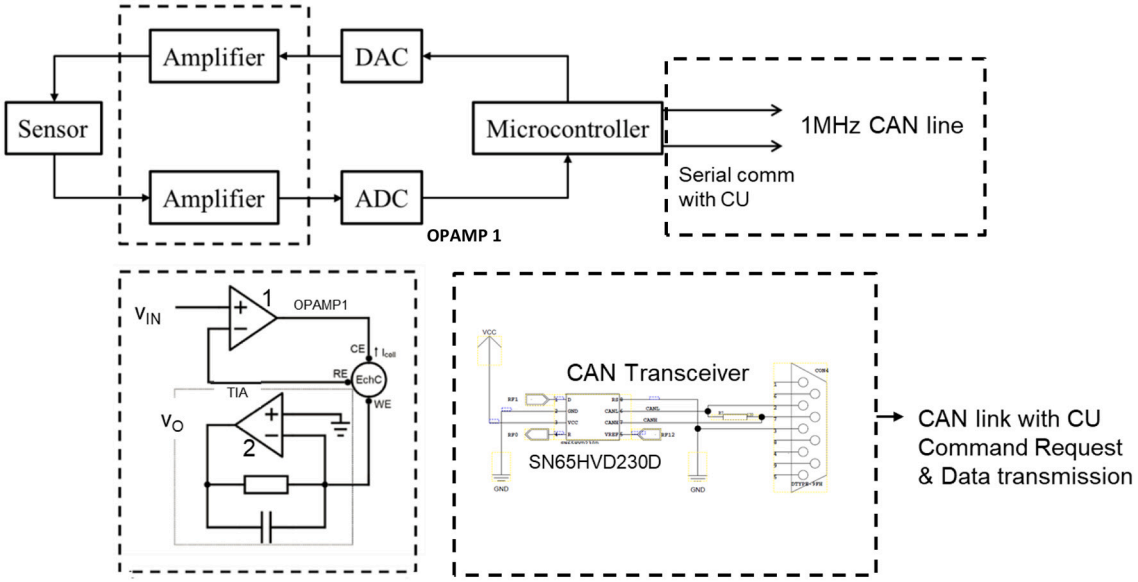

Fig. 6. Configuration schematic of the acquisition electronic system. The configuration of the OpAmp as a transimpedance amplifier (TIA) is shown inside the dotted region. The TIA consists of an OpAmp in inverter configuration, with a resistor converting the current (Icell) into a measurable voltage signal (Vout). A parallel capacitor acts as a low-pass filter to reduce both internal and external noise effects.

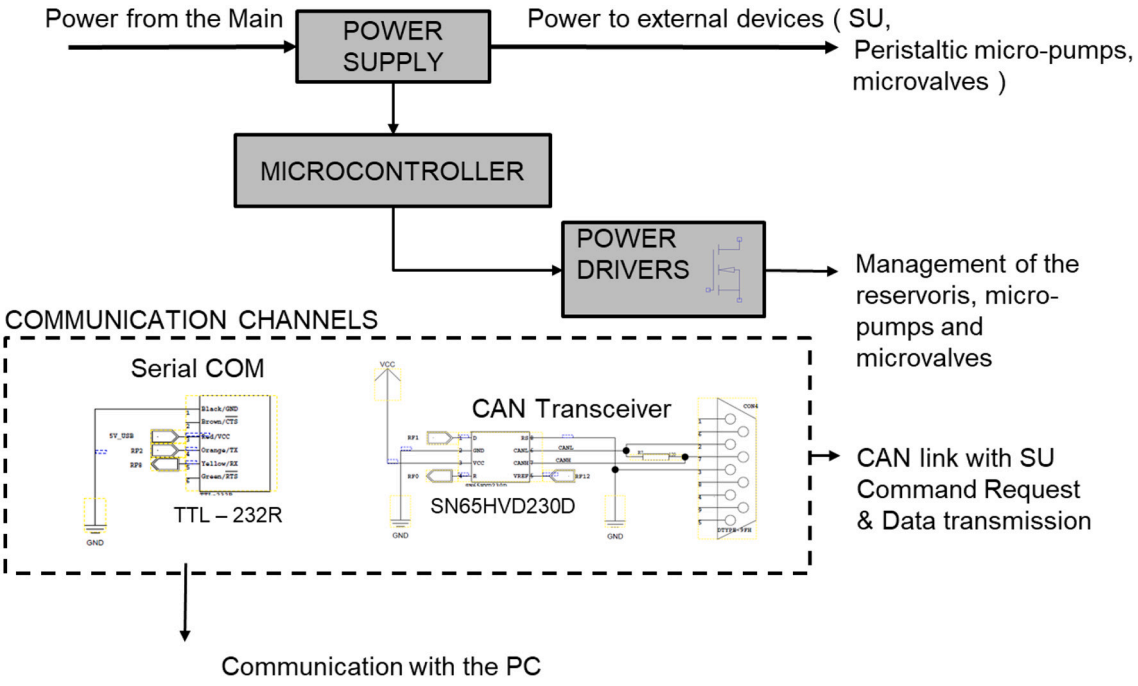

Fig. 7. Block diagram of the Central Unit. The main blocks are: (i) the supply system allowing to supply all system modules; (ii) the power drivers to manage micropumps, microvalves and reservoirs, and (iii) the communication subsystem to transmit commands and receive data with the Sensor Unit and the serial com to connect the whole device with the final user.

The first one is defined between the final user and the prototype. The user is connected to the platform using a final proprietary application software. This application allows to configure the measurement system, to plan timed measurements and to send data remotely. The communication between user and measurement system is based on the well-known RS232 serial communication protocol. The CU has a DB9 and a MAX232 transceiver that connects with the microcontroller's USART port. The communication protocol is embedded in the microcontroller and can be analyzed in Fig. S10. The connection with the PC is done using a FTDI TTL-232R-RPI. For more details, please see Fig. 7 and Figs. S3, S10 from the supplementary material.

The second communication protocol connects the CU and the SU. This communication is based on a 1 Mbs^{-1} CAN 2.0A protocol using a 2 MHz connection. The communication protocol between the CU and the SU (Fig. S10) permits to synchronize the measurement process between these two electronic systems. The CU will send CAN frames to the SU, indicating the end of the different states in the measurement process and will be waiting for the SU responses to either continue and start the new stage or repeat the transmission in case the response will be no ACK. Finally, in the stage where the mixing between antibodies and samples

has finished, the CU will send a request to start the pumping of the analyte and perform the measurement. When the measurement is done, the SU will send the response command to the CU, that will include the results of the measurement. Fig. 7 shows the block diagram of the CU, including the two communication transceivers: The MAX232 for the data transmission to the final user and the SN65HVD230D for the CAN communication with the SU. Fig. S10 shows the embedded firmware flow diagram for the management of the CU, including the aforementioned communication protocols and the management of the different microvalves and micropumps.

2.5. Analysis of the whole system's power consumption

The final prototype, with less than 1 kg of weight and packed in a volume of 2175 cm^3 is a real portable device that will permit to measure contaminants *in situ* and in real time. To analyze the power consumption of the device, we have (i) to consider the measurement process described in the previous sections, (ii) to know the quantities of liquids and interval times summarized in Table 1, and (iii) to know the power consumption of the different elements (microvalves, micropump, SU, CU, …), that can be obtained from its datasheets. With all this information, it is possible to calculate the energy consumption in a whole measurement procedure (a cycle).

The 24 VDC 064 Series ASCO microvalves (2.5 W of power consumption) are equipped with a special, optional integrated electronic component that reduces the energy consumption by 40% (Power Reduction Factor or PRF), which represents a final power consumption of 1 W. The Instech P625/900.143 micropump has a power consumption of 0.45 W (Supply voltage: 18 V and current: 25 mA). Indeed, due to the fact that the main supply for this system is 24 V, it means that there is a dissipation power of 0.15 W that must be added when the μPump is used. Anyway, in both cases (μVs and μPump), this consumption will take place during the period in which such devices are required. No quiescent current is considered due to the fact that power is cut by the CU when these devices are not in use. The CU electronic board has a power consumption of 0.288 W while the SU electronic board has a consumption of 0.185 W. Both board's power consumptions were estimated in lab.

Table 2 shows the Power dissipation per device, the measurement cycle time, approximately 1 h and 20 min, and the estimated energy consumption of the prototype. As can be observed from Table 2, the energy dispended to perform an automatic measurement will be 3.1234 W·h. This is 130.14 mA·h at 24 V. Analyzing the behavior per group of components we observe that the major consumption corresponds to those μValves associated with the Fluidic Module, approximately the 50% of the total. The Tanks μValves present a consumption of about 25% and the electronic boards around 15%. The peristaltic μPump has a consumption of about the 7.5% of the total energy and finally, the μValves that manage the pulsing fluidic method have a consumption per measurement cycle of about 3%.

3. Experimental details: sensor and sensing procedure

3.1. Reagents, material and instrumentation

Screen-printed Au electrodes (Au/SPEs DRP-8X220AT, Methrom Dropsens, Spain) consisting of a 2.5-mm smooth Au working electrode, an Au counter electrode and an Ag pseudo-reference electrode, were used. UV/Ozone Procleaner™ unit from Bioforce Nanoscience (Ames, IA, USA) was used to ensure the best possible electrodes cleaning. The calibration curves were fitted to a four-parameter logistic equation using the Graph Prism software (GraphPad Software, San Diego, CA, USA).

The immunoreagents used in this study (4e-BSA/As87) have previously been described for the detection of Irgarol 1051® [35,36,47]. The cross-reactivity profile of 4e-BSA/As87 assay was determined by ELISA obtaining the following values: Irgarol 100%, Atrazine 6.1%, Simazine 0.4%, Terbutryn 349.4%, Ametrine 23.8% and Melamine <0.03%. The antibody As87 and 4e-BSA have been performed with the support of the ICTS "NANBIOSIS", more specifically by the Custom Antibody Service (CAbS, CIBER-BBN, IQAC-CSIC). The secondary antibody peroxidase conjugate (AntiIgG–HRP) were purchased from Sigma (St. Louis, MI, USA). The O-(2-Carboxyethyl)-O′-(2-mercaptoethyl)-heptaethylene glicol (PEG-thiol-acid) and 2,5,8,11,14,17,20-Heptaoxadocosane-22-thiol (mPEG-thiol) were acquired from Polypure (Oslo, Norway). Stock solutions of Irgarol 1051® (10 mmol L^{-1}) was prepared in dimethyl sulfoxide (Merck) and stored at 4 °C. Phosphate-buffered saline (PBS) is 0.01 M phosphate buffer on a 0.8% saline solution, and the pH is 7.5. PBST is PBS with 0.05% Tween 20. For electrochemical measurements, it was used citrate buffer at 0.04 M, pH 5.5, and detection solution (DS) was also prepared containing 0.001% TMB (3,3′,5,5′-tetramethylbenzidine) and 0.0004% H2O2 in citrate buffer. The regeneration solution (RS) is 0.3 M sodium hydroxide.

The derivatization and functionalization of the working electrodes as well as the amperometric measurement was done as described [33]. Basically, the derivatization of the gold surface was addressed by the addition of mixed self-assembled monolayer (SAM) with a PEG-thiol-acid and mPEG-thiol. The immobilization of the coating antigen 4e-BSA was performed according to a previous work [31,32]. The gold SPEs were rinsed with organic solvent, cleaned using an UV/Ozone Procleaner™ and functionalized mixed self-assembled monolayer (m-SAM). Subsequently, the antigen 4e-BSA (100 μg ml^{-1} in PBS, 25 μl per SPE) were immobilized mixing with 25 μl containing the EDC/NHS (200 mM in PBS) and incubating for 3 h at RT. After this time, the SPEs were rinsed with PBS and capped. Finally, the biofunctionalized SPE chips were washed with water and stored in a desiccator until use.

3.2. Automatic immunosensor protocol

The device must work autonomously by executing analyte sample measurements in air conditions at predefined times. Other fundamental requirement for the device is the execution of:

1. An effective cleaning phase to prevent water intra-sample contamination, defined in steps 6, 8 and 10 Table 1.

Table 2
Estimated energy consumption of the whole prototype, including the microvalves (6 μVs) of the different reservoir tanks, the 3 μVs associated to the filling and emptying of the Fluidic Module (FM), the 9 μVs related with the pulsed flow method (PFM) and the micropump μP.

Devices	Biosensor	Tanks	FM	PFM	CU	SU	Total
	μP @1.6 ml/m	μVs	μVs	μVs	eBoard	eBoard	
W	0.45	2.5	2.5	2.5	0.288	0.185	3.1234 Wh
PRF	0.98	0.4	0.4	0.4	1	1	
W·h	0.2425	0.798	1.548	0.0833	0.389	0.062	
number	1	6	3	9	1	1	1 h:21'
time	24′:15"	–	–	2′:30"	1 h:21'	20′	

2. An exact, well timed, procedure to provide SU, hosting the biosensor, a mixture easily measured with high accuracy and other liquids to preserve its functionalities in the long working time.

The Initial procedure to perform before (steps (a) and (b)) and after (steps (c-e)) the measurement protocol described in Table 1 is the following:

a) Empty DT, fill up DT with PBST 8 ml, keep it inside 2 min,
b) Enter all DT content to SCs at 1.6 ml/min (5 min needed),
c) Add Regeneration Solution 8 ml at 1.6 ml/min ml/min in SCs (5 min needed),
d) Fill up DT with PBST 8 ml, keep it inside 2 min,
e) Enter all DT content to SCs at 1.6 ml/min, keep SCs flooded (5 min needed).

Prior to analysis, a sample (4 ml) were mixed with the antibody solution at proper concentration (As87 diluted 1/500 in PBST 4 ml). The mixture was flowed to the DT using the A-SW channel. Once all the sample volume is loaded in the DT, the protocol of the assay starts by transferring the content of the DT in the eight µchamber according the pulsed-flow method. After that, empty the biosensor µchambers followed by washing with PBST buffer (5 ml at 1.6 ml/min). Then, anti-IgG-HRP 8 ml were flowed through the biosensor followed by PBST washing. Finally, a substrate solution (DS tank) that contained the mediator for amperometric measurement was flowed through the sensing chamber. The response acquisition starts automatically after the addition of DS 3 ml. The cycle concludes with a new cleaning process consisting of PBST 5 ml. Then, Regeneration Solution (RS) 10 ml is flowed through the system at 1.6 ml/min to prepare the electrodes for the next measurement.

4. Results and discussion

In order to demonstrate the feasibility of the device, we have proposed the implementation of the immunoreagents for the determination of Irgarol 1051®, commonly named Cybutryne. Irgarol 1051® is one of the most employed antifouling agents and is one of the most commonly found in the marine environment [43].

4.1. Maximum signal response

Gold screen printed electrodes (Au SPE) were used to test the device performance according to good reproducibility, robustness and the regenerations as described in a previous work [31,32]. However, in this case, the used chip includes eight Au SPE that would allow the immobilization of up to eight different biomolecules. With the aim to demonstrate the performance and the reproducibility between the eight different Au SPE, the same biomolecule was immobilized.

The first test is to evaluate the behavior of the signal using pulsing method. Following the assay summarized in Fig. 1, the assay started by the addition of the specific As87antibody and after a period of time an aHRP solution was added. After that, the substrate solution was pumped in all the chambers and subsequently, the signal was acquired. From Fig. 8, the steady state of the signal has been reached after 120 s, approximately. However, a periodic decay signal convoluted with the sensor response were observed in the acquisition of the signal in all the channels. Also note the time shift among the different sensors associated with the channel activation. This behavior is in concordance with the pulsing method implemented in the device. The period observed is 8 s and a delay between channels of 1 s, as it was planned (see Fig. 8). The signal per channel obtained was from 0.8 and 1.0 with small variation within chamber (CV of 4.8 ± 1.1%). According to this low CV per channel, the last measurement was chosen to be used as final signal to be plotted. Thus, the mean value obtained in all the channels was 0.85 ± 0.06 r.u. (CV 7.3%).

We would like to highlight that all the experiments carried out in this work were performed with the same SPE 8× chip. The reproducibility of the test has been performed in four consecutive days measuring all channels at maximum signal. The results obtained a robust assay in terms of reproducibility between channels (from 4.5 to 8.5% of Coefficient of variation) as well in different days (Day1: 0.85 ± 0.06, Day2: 0.94 ± 0.04, Day3 0.69 ± 0.04 and Day4: 0.68 ± 0.07; mean ± SD from eight channels). Long-term analysis is out of the scope of this paper because it was not the objective of this work. However, taking into consideration the appropriate storage of the chip (usually immersed in a solution of PBS with 0.5% of BSA), we expect that stability will be high, but it should be tested in the future. Finally, it is important to remark that the chip was uninstalled every day and kept in the fridge at 4 °C, so the fact of installing and uninstalling have not affected to the signal response.

4.2. Immunosensor determination of Irgarol 1051®

Once it was demonstrated that our immunosensor acquired the immunochemical signal with low variability, it was decided to prove if our immunosensor is able to determine Irgarol 1051® in the same way that in ELISA [36] or using an static amperometric immunosensor [31,32]. Thus, different concentrations of Irgarol have been measured using the same chip and the last measurement of the whole chronoamperogram was recorded to be plotted in a graph (see Fig. 9). These sequential measurements were possible to be done with the same chip

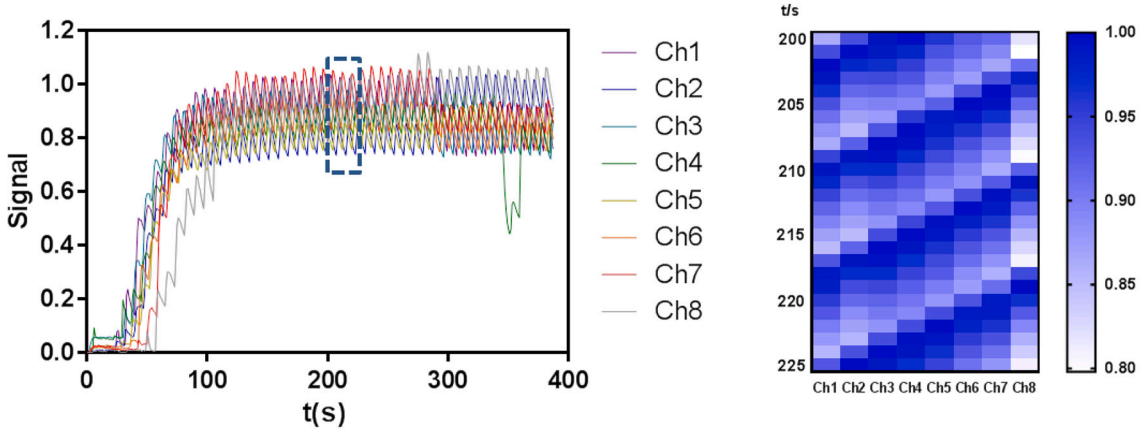

Fig. 8. (Left) Chronoamperogram corresponding to the acquisition of the maximum signal after the addition of the substrate solution. (Right) Heating map of the signal acquired within the acquisition window of 200–225 s.

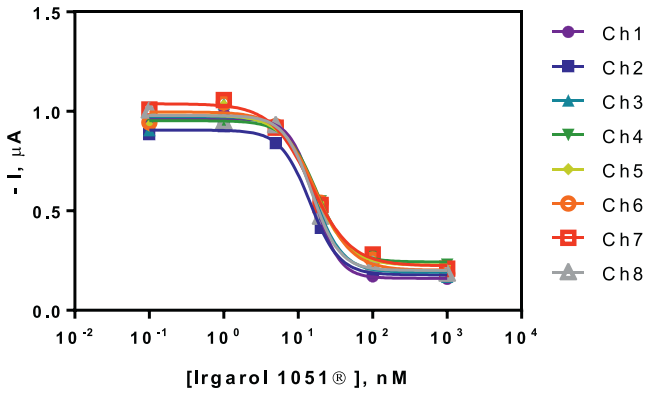

Fig. 9. Calibration curves obtained for the determination of Irgarol 1051® in the eight individual Au SPE using our measurement prototype.

due to a regeneration procedure that was applied in the whole immunosensor following the procedure- that was detailly explained in section 2.1, Table 1 and section 3.2.

As it can be observed in the Fig. 9, a low degree of variability was found in the different concentrations that were tested (CV 8.7 ± 4.8%). The four-parameter logistic fitting of each individual channel (see Table 3) gave a mean value of the IC50 of 16.0 ± 1.1 nM (4.1 ± 0.3 µg/l in buffer) with a CV of 7.2%. The limit of detection (LOD) was calculated also for all the channels and a LOD of 0.61 ± 0.13 nM (0.15 ± 0.03 µg/l in buffer) was reached. The detectability found was comparable to the previous work [44] which obtained an LOD of 0.15 ± 0.09 nM. The reproducibility of the maximum signal was evaluated measuring in four consecutive days. Values of 0.85 ± 0.06, 0.94 ± 0.04, 0.69 ± 0.04 and 0.68 ± 0.07 was found with a CV of 7.3, 4.6, 6.0 and 9.7%, respectively. Although some variability was found on different measurement days, the measurements continued to be in range. Good agreement between channels and low variability were also found.

Finally, it is important to consider two effects than can disturb the measurement work in a real scenario: (i) the stability of the different bioreagents involved in the measurement process and (ii) the effect of the temperature on the bioassay performance. The stability of antibodies is crucial to ensure the reproducibility of the immunosensor in a final device that will be isolated in the sea, with long time periods of autonomous work without the supervision of specialized personnel. In order to stabilize them, different additives such as trehalose or sucrose as well high salts concentrations may improve the stability of the antibody solution over time. On the other hand, Temperature is critical in any immunoassay and should be considered during the measurement process. Two possibilities can be considered. The first option is to maintain the temperature in the whole system. However, this control cost a lot of energy and is unsustainable in long time measurements for isolate devices. The second option consist on the minimization of this problem using one of the SPE as a reference channel to monitor antibody binding (similarly to control line in lateral flow immunoassay or commonly named rapid test).

Table 3
Analytical parameters from the eight calibration curves acquired simultaneously for the detection of Irgarol 1051®. A four-logistic equation was employed for the fitting of the data acquired. The mean value and SD correspond to the eight different SPE. Limit of detection (LOD) was calculated for each calibration curve to the IC90.

Analytical parameters	
-Imax, µA	0.974 ± 0.038
-Imin, µA	0.204 ± 0.027
Slope	−2.10 ± 0.32
IC_{50}, nM (µg/L)	16.0 ± 1.1 (4.1 ± 0.3)
R^2	0.995 ± 0.005
LOD, nM (µg/L)	0.61 ± 0.13 (0.15 ± 0.03)

4.3. A comparative analysis of our proposal versus alternative methodologies

Table 4 summarizes a comparison of different immunoassays developed using the same immunoreagents doing a critical comparison about characteristic features highlighted in a point-of-care devices. In general, chromatographic techniques [45,46] are the gold standard for the quantification and detection of pesticides, however the assay time is usually high because it requires a preconcentration step using solid phase extraction procedures (SPEP). SPEPs allows the clean-up of the matrix and preconcentrate the sample which is traduced in a better detectability (low sub-ppb). In comparison with the different immunoassay formats, ELISA is the most sensitive one [47], but it cannot be used in-field analysis. Both optical and electrochemical immunosensors developed [33,38] are quite similar in terms of detectability and with similar multiplexing capabilities, however the cost of the chip is substantially higher for the optical than the electrochemical. However, the fact that each chip can be regenerated and ready for the next measurement, makes that the assay/cost is lower. Our proposal improves the multiplexing capabilities regarding the way how the liquids are handling being feasible the automatization.

5. Conclusions

A low-cost, low-power miniaturized electrochemical device was designed, developed and tested for the *in-situ,* simultaneous monitoring of up to eight pollutants. The mechanical and fluidic system was designed to be interconnected with a matrix of eight biosensors in a compact, miniaturized and integrated way with the aim of minimizing the tubing and global encapsulation, integrating the different microvalves and peristaltic micropumps, and allowing the analysis of electrochemical amperometry for the different biosensors without any kind of interference between them. The prototype had a size of 10 × 10 × 20 cm3, with a final weight of 1 kg approximately (in empty condition).

The complete system design is flexible enough to leave a door open to fully autonomous operation and the application of various electrochemical techniques, such as amperometry, cyclic voltammetry, and electrochemical impedance spectroscopy, and future steps will consider remote data transmission through the Internet connection at tablets. The amperometry is the applied measurement technique, since currently it is the advanced state-of-the-art regarding precision, reliability and repeatability. We have been able to measure simultaneously up to eight biosensors by in time flow multiplexing according to the pulsing-flow method also described in this work. The implemented system allows an identical amount of functional liquid to flow through each µchamber in identical way during a determined time regardless of the continuous input flow rate from the peristaltic pump. Our device was tested by immobilizing 4e-BSA on a three electrodes SPE array with each biosensor isolated in µchambers where the binding of the specific antibody and the sample containing the chosen contaminant, Irgarol 1051®, happens. In order to detect the binding antigen-antibody interaction, a secondary antibody labeled with HRP was added to provide us the electrochemical signal after adding the corresponding substrate (H_2O_2 / TMB). Regenerable biosensors allowing multiple, sequential measurements is a main advantage of this measurement type. The detectability of the measurements carried out by our system is similar to that of the reported ELISA and other developed systems, with a precision error of around 5%, as well as a repeatability of the order of 90%.

The system has proven its worth in performing eight simultaneous (parallel) measurements for multiple analyte detection or for single measurement redundancy. The results suggest that the developed device could be useful and easily integrable in POC environments.

Table 4
Comparison of different analytical approaches for Irgarol 1051® determination.

	HPLC-MS	ELISA	Electrochemical immunosensor	Optical immunosensor	Our proposal
Detectability	0.1–0.2 ng/L	15 ng/L	37 ng/L	66 ng/L	150 ng/L
Assay time	High	Medium	Medium	Medium	Medium
Portability	Low	Low	Medium	Medium	High
Multiplexing capabilities	High	Medium	Medium	Medium	High
Cost/analysis	High	Low	Medium-low	Medium	Medium-low
Reference	[45,46]	[47]	[33]	[38]	

Declaration of Competing Interest

The authors declare the following financial interests/personal relationships which may be considered as potential competing interests:

Manel Lopez has patent #EP17382269 licensed to Elements Works S. L.

Acknowledgements

This work has been funded by funding agency EC project SEA-on-a-chip (FP7-OCEAN-2013-614168) and partially supported by the European Union's Horizon 2020 research and innovation programme under the Marie Sklodowska-Curie agreement No 712949 (TECNIOspring-PLUS) and from the Agency of Business Competitiveness of the Government of Catalonia (TECSPR18-1-0042). The Nb4D group is a consolidated research group (2017 SGR 1441).

Appendix A. Supplementary data

Supplementary data to this article can be found online at https://doi.org/10.1016/j.sbsr.2022.100505.

References

[1] J. Baten, A History of the Global Economy: 1500 to the Present, Cambridge University Press, Cambridge, 2016.
[2] J. Bostock, A. Lane, C. Hough, K. Yamamoto, An assessment of the economic contribution of EU aquaculture production and the influence of policies for its sustainable development, Aquac. Int. 24 (2016) 699–733.
[3] EC, Communication from the Commission to the European Parliament, the Council, the European Economic and Social Committee and the Committee of the Regions – Innovation in the Blue Economy: Realising the Potential of Our Seas and Oceans for Jobs and Growth COM(2014) 254 final/2, 2014.
[4] J. Guillen, F. Natale, J.M. Fernández Polanco, Estimating the economic performance of the EU aquaculture sector, Aquac. Int. 23 (2015) 1387–1400.
[5] EC. https://eceuropaeu/info/food-farming-fisheries_en, 2020 https://ec.europa.eu/jrc/en/news/eu-aquaculture-report-2020.
[6] M. Farré, L. Kantiani, M. Petrovic, S. Pérez, D. Barceló, Achievements and future trends in the analysis of emerging organic contaminants in environmental samples by mass spectrometry and bioanalytical techniques, J. Chromatogr. A 1259 (2012) 86–99.
[7] J.P. Salvador, J. Adrian, R. Galve, D.G. Pinacho, M. Kreuzer, F. Sánchez-Baeza, et al., Chapter 2.8 Application of bioassays/biosensors for the analysis of pharmaceuticals in environmental samples, in: M. Petrovic, D. Barceló (Eds.), Comprehensive Analytical Chemistry, Elsevier, 2007, pp. 279–334.
[8] M.-P. Marco, S. Gee, B.D. Hammock, Immunochemical techniques for environmental analysis. I. Antibody production and immunoassay development, Trends Anal. Chem. 14 (1995) 415–425.
[9] M.-P. Marco, S. Gee, B.D. Hammock, Immunochemical techniques for environmental analysis. I. Immunosensors, Trends Anal. Chem. 14 (1995) 341–350.
[10] L.S.A. Busa, S. Mohammadi, M. Maeki, A. Ishida, H. Tani, M. Tokeshi, Advances in microfluidic paper-based analytical devices for food and water analysis, Micromachines 7 (2016) 86.
[11] M.C. Cole, A.V. Desai, P.J.A. Kenis, Two-layer multiplexed peristaltic pumps for high-density integrated microfluidics, Sensors Actuators B Chem. 151 (2011) 384–393.
[12] A.M. Nightingale, A.D. Beaton, M.C. Mowlem, Trends in microfluidic systems for in situ chemical analysis of natural waters, Sensors Actuators B Chem. 221 (2015) 1398–1405.
[13] C. Dincer, R. Bruch, A. Kling, P.S. Dittrich, G.A. Urban, Multiplexed point-of-care testing – xPOCT, Trends Biotechnol. 35 (2017) 728–742.
[14] R.K. Gupta, R. Pandya, T. Sieffert, M. Meyyappan, J.E. Koehne, Multiplexed electrochemical immunosensor for label-free detection of cardiac markers using a carbon nanofiber array chip, J. Electroanal. Chem. 773 (2016) 53–62.
[15] G. Lai, F. Yan, H. Ju, Dual signal amplification of glucose oxidase-functionalized nanocomposites as a trace label for ultrasensitive simultaneous multiplexed electrochemical detection of tumor markers, Anal. Chem. 81 (2009) 9730–9736.
[16] N. Radha Shanmugam, S. Muthukumar, S. Chaudhry, J. Anguiano, S. Prasad, Ultrasensitive nanostructure sensor arrays on flexible substrates for multiplexed and simultaneous electrochemical detection of a panel of cardiac biomarkers, Biosens. Bioelectron. 89 (2017) 764–772.
[17] J.F. Rusling, Multiplexed electrochemical protein detection and translation to personalized cancer diagnostics, Anal. Chem. 85 (2013) 5304–5310.
[18] C. Zhao, X. Liu, A portable paper-based microfluidic platform for multiplexed electrochemical detection of human immunodeficiency virus and hepatitis C virus antibodies in serum, Biomicrofluidics 10 (2016), 024119.
[19] M.S. Finch, D.J. Hydes, C.H. Clayson, W. Bernhard, J. Dakin, P. Gwilliam, A low power ultra violet spectrophotometer for measurement of nitrate in seawater: introduction, calibration and initial sea trials, Anal. Chim. Acta 377 (1998) 167–177.
[20] K.S. Johnson, L.J. Coletti, In situ ultraviolet spectrophotometry for high resolution and long-term monitoring of nitrate, bromide and bisulfide in the ocean, Deep-Sea Res. I Oceanogr. Res. Pap. 49 (2002) 1291–1305.
[21] K.S. Johnson, L.J. Coletti, F.P. Chavez, Diel nitrate cycles observed with in situ sensors predict monthly and annual new production, Deep-Sea Res. I Oceanogr. Res. Pap. 53 (2006) 561–573.
[22] K.S. Johnson, S.C. Riser, D.M. Karl, Nitrate supply from deep to near-surface waters of the North Pacific subtropical gyre, Nature 465 (2010) 1062–1065.
[23] I. Klimant, V. Meyer, M. Kühl, Fiber-optic oxygen microsensors, a new tool in aquatic biology, Limnol. Oceanogr. 40 (1995) 1159–1165.
[24] T.R. Martz, J.G. Connery, K.S. Johnson, Testing the Honeywell Durafet® for seawater pH applications, Limnol. Oceanogr. Methods 8 (2010) 172–184.
[25] N.P. Revsbech, An oxygen microsensor with a guard cathode, Limnol. Oceanogr. 34 (1989) 474–478.
[26] Y. Takeshita, T.R. Martz, K.S. Johnson, A.G. Dickson, Characterization of an ion sensitive field effect transistor and chloride ion selective electrodes for pH measurements in seawater, Anal. Chem. 86 (2014) 11189–11195.
[27] C.D.M. Campos, J.A.F. da Silva, Applications of autonomous microfluidic systems in environmental monitoring, RSC Adv. 3 (2013) 18216–18227.
[28] A. Jang, Z. Zou, K.K. Lee, C.H. Ahn, P.L. Bishop, State-of-the-art lab chip sensors for environmental water monitoring, Meas. Sci. Technol. 22 (2011), 032001.
[29] J.C. Jokerst, J.M. Emory, C.S. Henry, Advances in microfluidics for environmental analysis, Analyst 137 (2012) 24–34.
[30] G. Mills, G. Fones, A review of in situ methods and sensors for monitoring the marine environment, Sens. Rev. 32 (2012) 17–28.
[31] P. Fruhmann, A. Sanchis, L. Mayerhuber, T. Vanka, C. Kleber, J.-P. Salvador, et al., Immunoassay and amperometric biosensor approaches for the detection of deltamethrin in seawater, Anal. Bioanal. Chem. 410 (2018) 5923–5930.
[32] J.P. Salvador, M.P. Marco, Amperometric biosensor for continuous monitoring Irgarol 1051 in sea water, Electroanalysis 28 (2016) 1833–1838.
[33] J.-P. Salvador, K. Kopper, A. Miti, A. Sanchis, M.-P. Marco, Multiplexed immunosensor based on the amperometric transduction for monitoring of marine pollutants in sea water, Sensors 20 (2020) 5532.
[34] B. Ballesteros, D. Barceló, F. Camps, M.-P. Marco, Enzyme-linked immunosorbent assay for the determination of the antifouling agent Irgarol 1051, Anal. Chim. Acta 347 (1997) 139–147.
[35] B. Ballesteros, D. Barcelo, F. Sanchez-Baeza, F. Camps, M.-P. Marco, Influence of the Hapten design on the development of a competitive ELISA for the determination of the antifouling agent Irgarol 1051 at trace levels, Anal. Chem. 70 (1998) 4004–4014.
[36] N. Sanvicens, B. Varela, B. Ballesteros, M.P. Marco, Development of an immunoassay for terbutryn: study of the influence of the immunization protocol, Talanta 89 (2012) 310–316.
[37] A. Sanchis, J.P. Salvador, K. Campbell, C.T. Elliott, W.L. Shelver, Q.X. Li, et al., Fluorescent microarray for multiplexed quantification of environmental contaminants in seawater samples, Talanta 184 (2018) 499–506.
[38] B. Chocarro-Ruiz, S. Herranz, A. Fernández Gavela, J. Sanchís, M. Farré, M. P. Marco, et al., Interferometric nanoimmunosensor for label-free and real-time monitoring of Irgarol 1051 in seawater, Biosens. Bioelectron. 117 (2018) 47–52.
[39] M.A. Gonzalez-MartInez, J. Penalva, R. Puchades, A. Maquieira, B. Ballesteros, M. P. Marco, et al., An Immunosensor for the automatic determination of the antifouling agent Irgarol 1051 in natural waters, Environ. Sci. Technol. 32 (1998) 3442–3447.
[40] M. Suzuki, H. Akaguma, Chemical cross-talk in flow-type integrated enzyme sensors, Sensors Actuators B Chem. 64 (2000) 136–141.
[41] J. Wu, Z. He, Q. Chen, J.-M. Lin, Biochemical analysis on microfluidic chips, TrAC Trends Anal. Chem. 80 (2016) 213–231.

[42] B.E.-F. de Ávila, V. Escamilla-Gómez, S. Campuzano, M. Pedrero, J.M. Pingarrón, Disposable electrochemical magnetoimmunosensor for the determination of troponin T cardiac marker, Electroanalysis 25 (2013) 51–58.
[43] I.K. Konstantinou, T.A. Albanis, Worldwide occurrence and effects of antifouling paint booster biocides in the aquatic environment: a review, Environ. Int. 30 (2004) 235–248.
[44] J.-P. Salvador, M.-P. Marco, Amperometric biosensor for continuous monitoring irgarol 1051 in sea water, Electroanalysis 28 (2016) 1833–1838.
[45] M.H. Lamoree, C.P. Swart, A. van der Horst, B. van Hattum, J. Chromatogr. A 970 (2002) 183–190.
[46] Á. Sánchez-Rodríguez, Z. Sosa-Ferrera, Á. Santana-del Pino, J.J. Santana-Rodríguez, Mar. Pollut. Bull. 62 (2011) 985–991.
[47] A. Sanchis, C. Bosch-Orea, J.P. Salvador, M.P. Marco, M. Farré, Anal. Bioanal. Chem. 411 (2019) 5897–5907.